Heliyon 5 (2019) e01924

Contents lists available at ScienceDirect

Heliyon

journal homepage: www.heliyon.com

Similarities and differences for atomic and diatomic molecule adsorption on the B-5 type sites of the HCP(10$\bar{1}$6) surfaces of Co, Os, and Ru from DFT calculations

Rees B Rankin *

Department of Chemical Engineering, Villanova University, WH 313, 800 E Lancaster Ave, Villanova, 19085, PA, USA

ARTICLE INFO

Keywords:
Nanotechnology
Energy engineering
Chemical engineering
Theoretical chemistry
Physical chemistry
Materials chemistry
Materials science
Metallurgical engineering

ABSTRACT

The differences in relative adsorption energies for mono-atomic and diatomic prototype species (C,N,O,S,H,-CO,NO,SO,CH,NH,H_2,O_2) relevant to catalytic processes such as Fischer-Tropsch and Ammonia Synthesis chemistry are investigated on the previously un-studied (10$\bar{1}$6) surface(s) of Co, Os, and Ru. Recent work in the literature has confirmed that catalytically relevant nanoparticles of HCP elements such as Co, Os, and Ru typically possess highly active 'B5' sites; unfortunately many early and extant theory and model-ing treatments of "stepped HCP surfaces" use *ad-hoc* created steps via manual deletion of atoms from an ideal HCP(0001) slab model. To date the differences in adsorption energies at various B5 step edge types, and any possible trends across the same type of B5 sites on various HCP catalyst species has not been thoroughly characterized. Our work in this manuscript uses the low energy (10$\bar{1}$6) Miller Index surface of Co, Os, and Ru which exposes 2 distinct and strongly adsorbing step edge sites, the B5B and B5A step edge which have been reported as relevant in the literature for Cobalt nanoparticle catalysis applications. Results from this study should be used to help further understand atomistic processes on the stepped surfaces of catalytically active HCP elements.

1. Introduction

Contributing factors such as population growth, climate change, and rising demands for standards of living drive the need for research to increase abundant energy and commodity chemicals generated or synthesized from efficient chemical routes and using low-cost, sustainable catalyst technologies. Computational modeling methods and tools, particularly quantum chemistry and related software, continue to become more relevant yearly as in-creases in computing power bring larger and more realistic system models for calculations into economic or feasible considerations. An area where this latter fact is leveraged heavily in the recent decade is the computational catalysis community interested in heterogeneous reactions. Larger surface slab models, explicit solvent molecules, and Van der Waals correc-tions are among typical improvements made for DFT calculations to increase the accuracy of the system model to the realistic material being simulated. Such advances will be key to bringing Rational Materials Design to realistic fruition, however there is still much work to do first in characterizing fundamental atomistic processes and properties on many catalyti-cally relevant materials as it has been shown that scaling relations and Volcano Plots may be more generalizable yet complicated than initially assumed [1, 2, 3, 4, 5, 6].

Among the group of inner d-block transition metal catalysts for a variety of reactions are elements including Cobalt, Osmium, and Ruthenium. Cobalt is an active catalyst for reactions such as Fischer-Tropsch (FT) synthesis and Dry Reforming of CH_4, Osmium a relatively mediocre catalyst for alkene hydroxylation and the Haber-Bosch reaction and a good doping/alloying agent in making intermetallic Oxygen Reduction Reaction (ORR) catalysts, and Ruthenium an active catalyst for FT synthesis, Haber-Bosch and recently in biofuels conversion [7, 8, 9, 10, 11, 12, 13, 14, 15, 16]. Despite the fact these materials have been used and researched for such catalytic applications for decades, only recently has there been a large uptick in research related to understanding exact atomic mechanisms for their catalytic properties via the step and edge sites that their nanoparticles possess [7, 8, 17, 18, 19, 20, 21, 22, 23, 24, 25, 26].

Previous computational and theory studies of the adsorption energies and catalytic prop-erties of Co,Os, and Ru materials have typically relied on using over-simplified surface models of the step sites that HCP catalyst nanoparticles of these elements possess. In particular, such models typically involve using the HCP(0001) surface and either adding or de-

* Corresponding author.
E-mail address: rb.rankin@villanova.edu.

https://doi.org/10.1016/j.heliyon.2019.e01924
Received 4 March 2019; Received in revised form 27 May 2019; Accepted 5 June 2019

leting atoms along linear surface rows to create pseudo-step edges [7, 10, 14, 17, 18, 22, 27, 28]. This work was most likely done for a combination of reasons, but among them is typically the relatively small calculation cell size and economy of the calculation. An unfortunate drawback of this approach is that it creates only one type of step edge and associate site(s) around the step edge. However, other work has shown that in fact the nanoparticles of real catalysts of these elements have small amounts of (0001) and other low index facets and have large percentages of step and step-related facets and facet-intersections [8, 25, 26]. The surface energy of various HCP facets was previously examined in small detail in the literature, and among the lowest energy Milled Index HCP surfaces identified could be the HCP $(10\bar{1}6)$ surface. To date, this surface index has not been thoroughly characterized in the literature. The reasons for this absence could be compounded by factors including a large calculation cell which makes it expensive to treat via computation/modeling, and the rela-tively similar Miller Index (1015)which *may* express higher occurrence via Wulff construction or real surface formation thermodynamics dynamics [8, 18, 19, 20, 24].

The HCP$(10\bar{1}6)$ surface however is nonetheless very interesting and should be used as a computational tool for modeling adsorption and catalysis on stepped HCP surface for the following reasons moderately wide terraces (high step edge density), multiple step-edge types in a single calculation cell, and low surface formation energy (could be present on certain sized nanoparticles) [24]. In the work presented in this manuscript, we present results for comparing and contrasting trends and differences in the adsorption energies of small mono-atomic and diatomic species on the Co, Os, and Ru $(10\bar{1}6)$ surfaces. Our analysis shows that there is a marked difference for the adsorption energy on the differing B5–B and B5-A step edge site types, which can vary by up to 1 eV or more. This is common across all of the three HCP elements studied. Our results also indicate that for many of the species studied, both mono-atomic and diatomic, that the strongest adsorbing surface step edge is the $(10\bar{1}6)$B5–B and the lowest energy adsorption site(s) is/are usually the site(s) 2 and/or 4.

2. Methods

In this work, plane-wave Density Functional Theory (DFT) calculations were performed to study the adsorption energetics of mono-atomic and diatomic molecular species on the representative HCP$(10\bar{1}6)$ surfaces of the transition metals Co, Os, and Ru. Details of the calculations are presented in the sub-section §2.1 that follows. Details and figures depicting the slab models and adsorptions sites are provided in the second sub section §2.2 that follows.

2.1. Calculation details

Calculations that are described in the work presented in this manuscript were performed in the manner as described as follows. All calculations were performed using the Vienna Ab Initio Simulation Package (VASP), v 5.4 as implemented in MedeA v 2.21 from the Materials Design company [29, 30, 31, 32, 33, 34]. Plane-wave DFT calculations were performed with VASP through Medea as described above. Because of the wide range of species studied as adsorbates in this work (C,N,O,S,H,CO, NO,SO,CH,NH,H_2,O_2) , the rPBE-GGA functional was chosen. This functional may present absolute adsorption energies which are smaller than those known experimentally, however for this work we are interested in trends and differences in relative adsorption energy differences between sites and surfaces [35]. Geometries were relaxed for the adsorbate atoms and the top 3Å of the surface models (described in the next sub-section and paragraph(s)) to net forces less than 0.03 eV/Å. Relaxation of the electronic wavefunctions was performed until convergence of at least 10^{-6} eV was obtained. Smearing of the electronic wavefunctions near the Fermi Energy was treated with the Methfessel-Paxton 2*nd* order algorithm with a value of 0.2 eV [36].

Plane-waves were expanded to a cutoff energy of 520 eV, and spin-polarization was allowed for all calculations reported in this work. Expansion of plane-waves to this energy provided an energy cutoff at least 20% larger than the default in the pseudopotential for any elemental species included in this work. Electronic convergence with expansion past this cutoff energy yielded net differences in adsorption energy for the following test species C*, O*, S* of less than 0.005 eV. Accordingly, the choice to use 520 eV was made as sufficient for the sake of this work. K -point sampling was performed using a $2 \times 2 \times 1$ γ-centered grid for initial relaxation of the atomic positions (to 0.055 eV/Å); the grid was refined to $3 \times 3 \times 1$ spacing for further relaxation (0.030eV/Å) and more accurate energetic determination. Tests showing further refinement of both the k -point spacing or the plane-wave cutoff energy yielded results which indicate results that would not affect our conclusions by more than 1–2% in the relative adsorption energy differences. Initial convergence tests for inclusion of VdW corrections for long-range dispersion using the opt-rPBE functional indicated similar changes in relative adsorption energies of ~1–2%; we note that at the time this work was initiated this VdW DFT functional did not appropriate reproduce the bulk properties of Osmium. For this reason combined with the described minor impact on the relative adsorption energy differences, to be consistent in our treatment of all the materials' surfaces in this work, the non-VdW corrected functional was used. (A more detailed examination of the effects of VdW vs non-VDW absolute adsorption energies with this and other functionals will be the basis of future work that is currently underway.

2.2. Slab model and adsorption sites

Slab models used in this work and shown in Fig. 1 were placed in the vertical center of the calculation supercell which had a total 'height' of 28

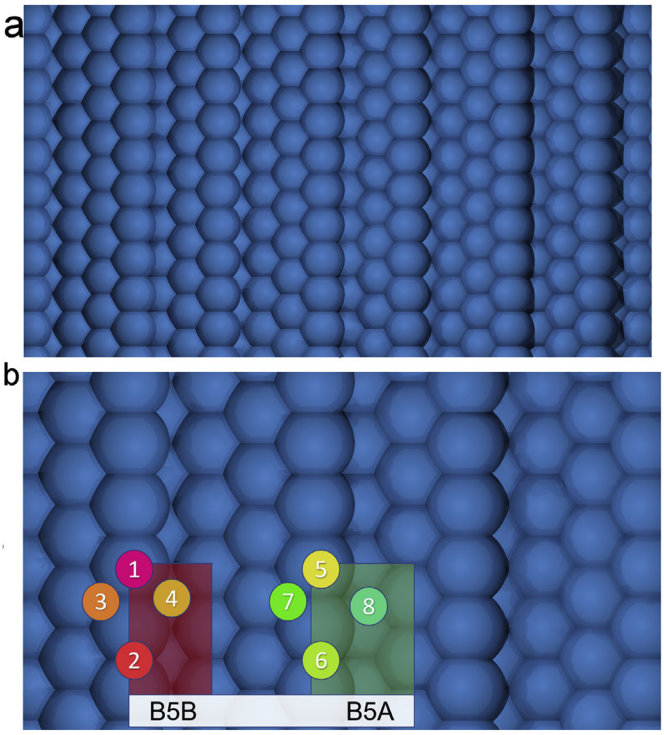

Fig. 1. Top-down views of the Co,Os, and Ru (10–16) surfaces. a) Extended view of multiple surface cells. b) Zoomed in view with semi-transparent boxes showing the two step edge types, and color-coded adsorption sites (color convention to plots in Figs. 3, 4, 5, and 6 and Figures SI.3 and SI.4 ('rankin-hcp-heliyon-SI.pdf ').

Å; this affords approximately 20 Å of vacuum spacing. For all surface slab models, the bulk lattice constant obtained using the same functional and cutoff energy for each element was used. A surface supercell was created with a p (1×3) periodicity from the primitive surface cell. Dipole corrections parallel to the surface normal were applied to reduced spurious interactions between slabs. For the specific DFT calculations described in this manuscript, calculation slabs of equivalent 'thickness' to a 5 layer (0001) slab were constructed. Adsorption sites for mono-atomic and diatomic molecular adsorbates are depicted in Fig. 2 below. As can be seen in Fig. 1 (b) and Fig. 2, there are 4 high-symmetry sites around each step edge which were sampled. Sites are given a label/numbering convention in Fig. 1 which is used consistently throughout the remainder of this manuscript including in Fig. 2. As can be seen in Fig. 1 (b) the surface contains 2 unique types of step edge (and hence, step site type) within each surface unit cell-these include a B5A and a B5B type site [8, 24]. Asymmetric diatomic adsorbates (CO, etc) were placed over the sites with the more electron-deficient species closer to the surface; symmetric diatomic adsorbates (H_2, O_2) were placed both horizontally and vertically centered over the site(s). For the symmetric diatomic adsorbates, placement of the molecules horizontally above the sites 1,2, and 5 introduced internal bond length elongations of >2% (but not fully dissociated molecules {criterion of 10% elongation or more}) on all of the Co, Os, and Ru surfaces. This indicates these sites might be active for the nearly-barrierless dissociation of these molecules on the surfaces, though the dissociated mono-atomic species produced therein may have a thermodynamic driving force to diffuse to other sites on or around the step-edge. For none of the asymmetric diatomic species studied was there any significant bond elongation on any of the sites studied in this work. (The activation and dissociation of these species will become the subject of future work that builds on this manuscript.)

3. Results and discussion

3.1. Trends on the Co$(10\bar{1}6)$surface

The results for studies of the adsorption energy of the species (C^*,N^*,O^*,S^*,H^*,CO^*,NO^*, SO^*,CH^*,NH^*,H_2^*, and O_2^*), $\Delta E ads_i$, is presented in Fig. 3 for the Co $(10\bar{1}6)$ surface. In this figure, results are binned by species and by site. A convention of 0 eV for the adsorption energy of that species indicates that it is the lowest energy adsorption site for that species identified in this work. Statistical Analysis of the results for the adsorption energies of the species is presented in the *Supplementary Information* Table SI.1 ('rankin-hcp-heliyon-SI.pdf ').

Several common features can be observed in Fig. 3 and Table SI.1 for the adsorption energies of the species in this work as studied on the Co $(10\bar{1}6)$ surface. First, the most common lowest energy binding site (s) was site 2 and 4, and the most common highest energy binding site was site 1. For 10 of the 12 the species studied, adsorption on the B5–B type step was more energetically preferred compared to the B5-A type step at the lowest energy site for each step type. The average difference in the lowest binding energy on each step type was -0.23 eV with a standard deviation of 0.44 eV with the B5–B step edge preference indicating a negative sign convention.

Among the species studied on this surface, the species least sensitive to the possible binding site(s) were: H, and CO. Among the species most sensitive to the possible binding site(s) were: C, SO, N, and CH. These results point to the fact that dissociation of larger adsorbate moieties such as HCOOH, hydrocarbons, NO_x, or SO_x on the step edge might be highly sensitive to which step edge a CO nanoparticle possesses and its abundance on the overall nanoparticle surface.

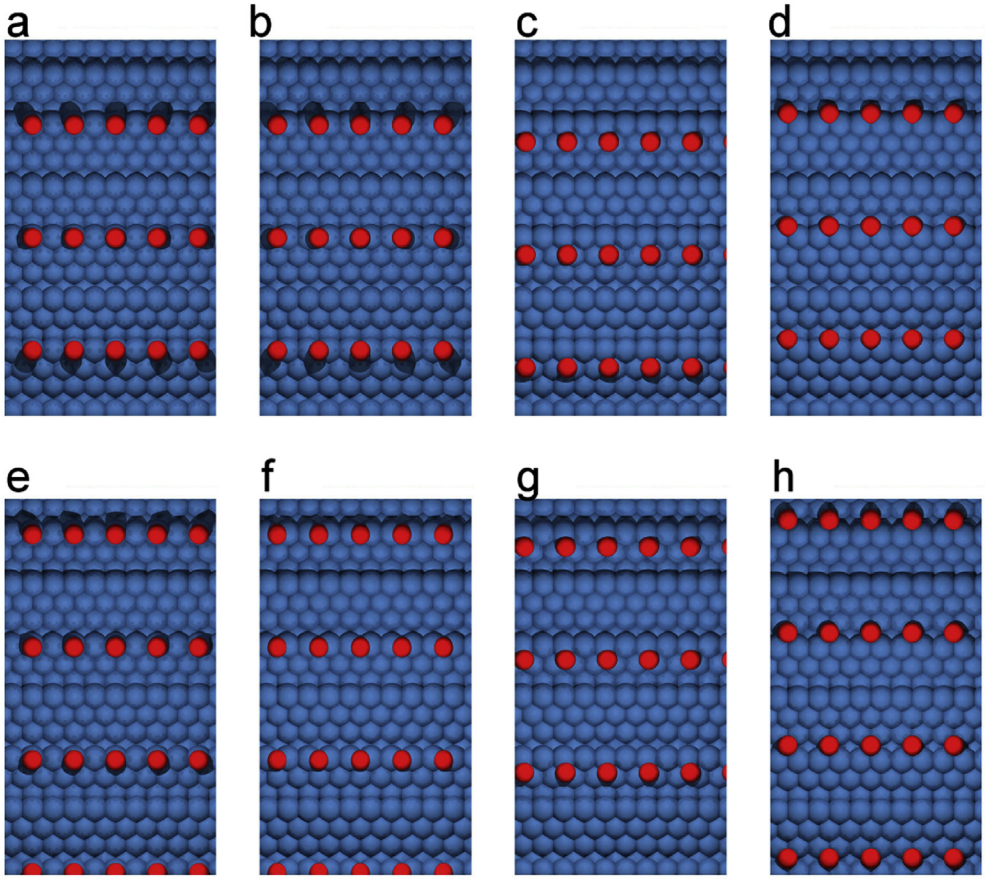

Fig. 2. Top-down views of the high-symmetry adsorption sites studied on the Co,Os, and Ru $(10\bar{1}6)$ surfaces. Sites 1 through 8 (as described in Fig. 1), given as panels a) through h), respectively. Prototypical adsorbate shown in red, surface atom in blue.

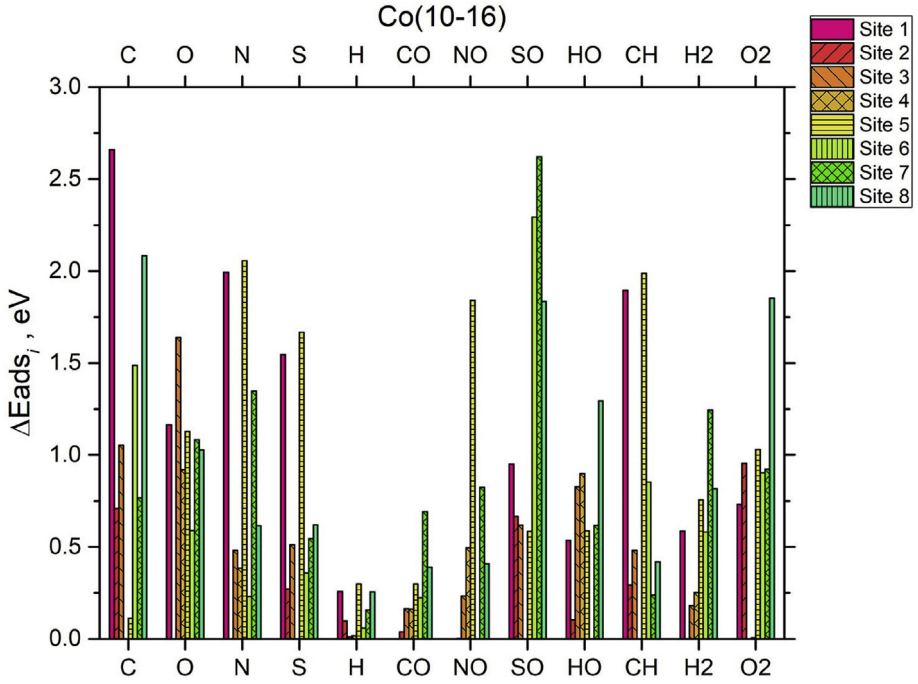

Fig. 3. Bar chart of relative adsorption energies, $\Delta E ads_i$, in eV, for the species studied in this work on the Co (10–16) surface. Data are grouped by adsorbate and site type.

3.2. *Trends on the Os*$(10\bar{1}6)$*surface*

The results for studies of the adsorption energy of the species (C^*,N^*,O^*,S^*,H^*,CO^*,NO^*, SO^*,CH^*,NH^*,H_2^*, and O_2^*), $\Delta E adsi$, are presented in Fig. 4 for the Os $(10\bar{1}6)$ surface. In this figure, results are binned by species and by site. A convention of 0 eV for the adsorption energy of that species indicates that it is the lowest energy adsorption site for that species identified in this work. Statistical Analysis of the results for the adsorption energies of the species is presented in *Supplementary Information* Table SI.2 ('rankin-hcp-heliyon-SI.pdf ').

Several common features can be observed in Fig. 4 and Table SI.2 for the adsorption energies of the species in this work as studied on the Os $(10\bar{1}6)$ surface. First, the most common lowest energy binding site was site 6 and then 2/4, and the most common highest energy binding site was 1,3, and 5. For 8 of the 12 species studied, adsorption on the B5– B type step was more energetically preferred compared to the B5-A type step. The average difference in the lowest binding energy on each step type was -0.11 eV with a standard deviation of 0.75 eV.

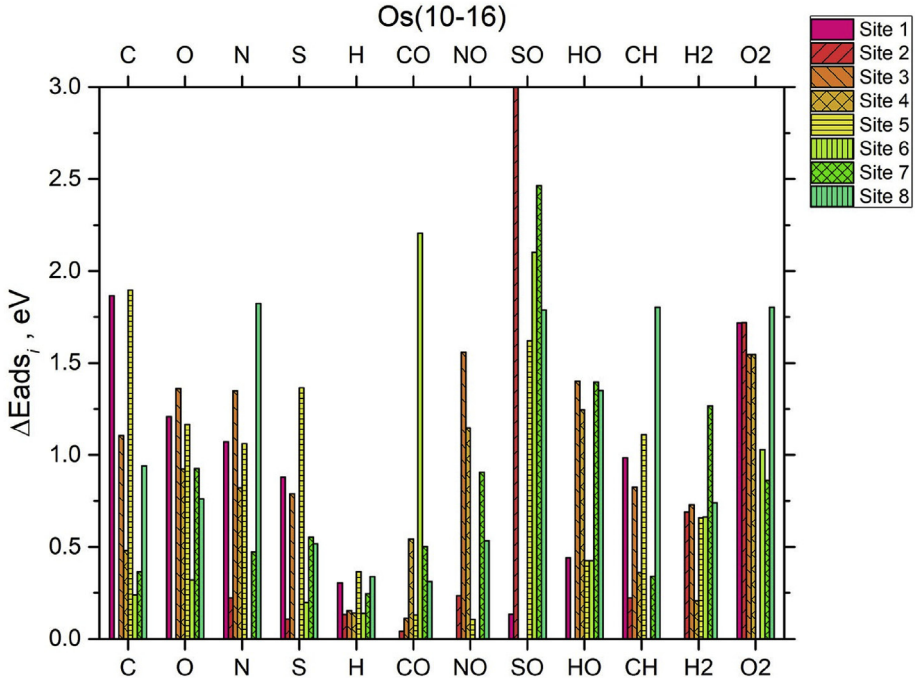

Fig. 4. Bar chart of relative adsorption energies, $\Delta E ads_i$, in eV, for the species studied in this work on the Os (10–16) surface. Data are grouped by adsorbate and site type.

Among the species studied on this surface, the species least sensitive to the possible binding site(s) were: H, and OH. Among the species most sensitive to the possible binding site(s) were: C, N, SO, CO, and H_2. These results also point to the fact that dissociation of larger adsorbate moieties such as HCOOH, hydrocarbons, NO_x, or SO_x on the step edge might be highly sensitive to which step edge a CO nanoparticle possesses and its abundance on the overall nanoparticle surface; this is particularly important of molecular hydrogen is a critical reactant in a catalytic process. The site/step sensitivity for its adsorption (via implication of BEP relation) indicates dissociation and poisoning of the step edge by H* may hinder the surface for some catalytic processes.

3.3. Trends on the *Ru*$(10\bar{1}6)$*surface*

The results for studies of the adsorption energy of the species (C^*,N^*,O^*,S^*,H^*,CO^*,NO^*, SO^*,CH^*,NH^*,H_2^*, and O_2^*), ΔE_{adsi}, is presented in Fig. 5 for the Ru $(10\bar{1}6)$ surface. In this figure, results are binned by species and by site. A convention of 0 eV for the adsorption energy of that species indicates that it is the lowest energy adsorption site for that species identified in this work. Statistical Analysis of the results for the adsorption energies of the species is presented in *Supplementary Information* Table SI.3 ('rankin-hcp-heliyon-SI.pdf ').

Several common features can be observed in Fig. 5 and Table SI.3 for the adsorption energies of the species in this work as studied on the Ru $(10\bar{1}6)$ surface. First, the most common lowest energy binding site (s) was site 6 then site 2 and 4, and the most common highest energy binding site(s) was site 1 and 5. For 5 of the 12 the species studied, adsorption on the B5–B type step was more energetically preferred compared to the B5-A type step at the lowest energy site for each step type; for 4 of the species the minimum on each type of step edge was essentially iso-energetic within the accuracy of the calculations presented in this work. The average difference in the lowest binding energy on each step type was -0.25 eV with a standard deviation of 0.54 eV with the B5–B step edge preference indicating a negative sign convention.

Among the species studied on this surface, the species least sensitive to the possible binding site(s) were: H, and CO. Among the species most sensitive to the possible binding site(s) were: C, S, N, and O_2. These results point to the fact that dissociation of larger adsorbate moieties such as HCOOH, hydrocarbons, NO_x, or SO_x on the step edge might be generally facile for many reaction pathways unless the moieties are dehydrogenated or de-oxygenated down to base elemental mono-atomic adsorbates such as C*, S*, or N*. This might help explain why Ru catalyst nanoparticles are generally robust and useful for many catalytic processes at many conditions; stepped Ru surfaces have previously been reported to be useful in a variety of catalytic applications as previously referenced in the introduction.

3.4. Trends across all surfaces: *Co* $(10\bar{1}6)$, *Os*$(10\bar{1}6)$, *Ru*$(10\bar{1}6)$

For all of the HCP metals studied, there were several trends observed that were common to all of their surface(s). Data has been plotted in several different forms to help guide the observations of interest: specifically Fig. 6 and Figs. SI.3 and SI.4 are given as sets of bar charts where the relative adsorption energies discussed are separated by surface, by site, and by species, respectively. For space, only Fig. 6 is shown in the main manuscript. (Please see the Supplementary Information 'rankin-hcp-heliyon-SI.pdf 'for the others.) The first observed trend is that as a predictive rule, adsorption on the step edge or the B5 site is preferable to that of the terrace site behind the step edge. This holds true for both the B5–B and the B5-A type step edges. As can be seen in Fig. 6 and Figures SI3 and SI.4, there are 2 small exceptions to this rule. The next observed trend is that for the mono-atomic adsorbates (C,H,N,S,O) the relative ordering of the energetic penalty to not bond on the site 2 or site 4 but instead atop a single atom of the B5–B step edge goes as CO > OS > RU. For the B5-A step edge there is no similar trend; if anything the trend is nearly reversed. The adsorption on the terrace like sites (3,7) of the B5–B and B5-A step edges also reveals an observation for the mono-atomic adsorbates: adsorptions on the B5-A related terrace is approximately 0.25 eV more preferable than the corresponding site on the B5–B type terrace sites. For the diatomic adsorbates, the first observed trend is that for the asymmetric species, adsorption around the B5–$_B$ step edge in general is much preferred compared to the B5-A step edge; some exceptions include species on Osmium, and SO* in general. H_2, CH, and OH behave both qualitatively and quantitatively similarly at the same site(s)

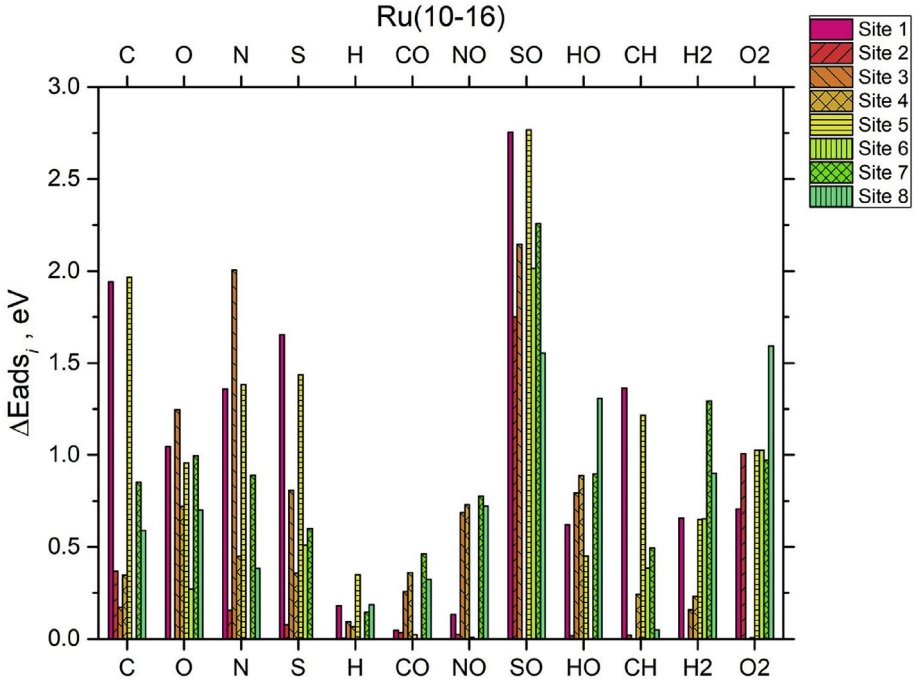

Fig. 5. Bar chart of relative adsorption energies, ΔE_{ads_i}, in eV, for the species studied in this work on the Ru (10–16)surface. Data are grouped by adsorbate and site type.

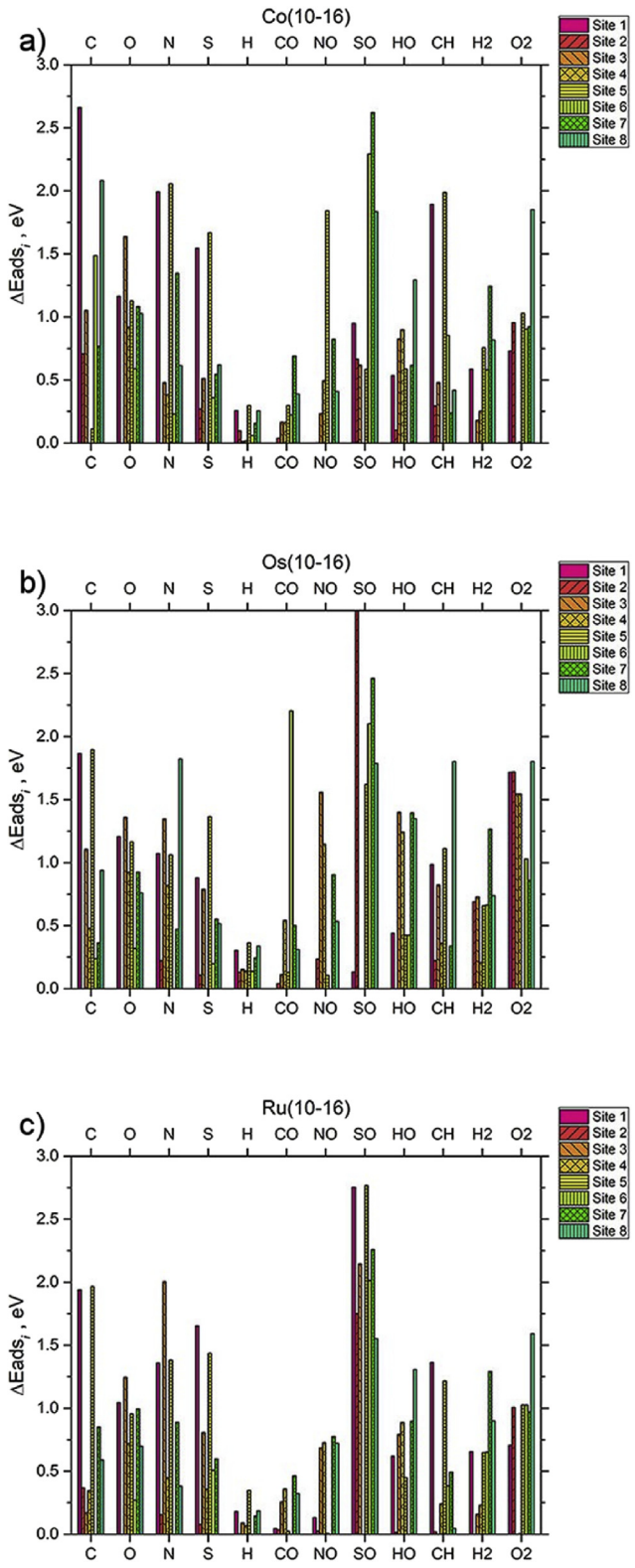

Fig. 6. Multiple Bar charts of relative adsorption energies, $\Delta E ads_i$, in eV, for the species studied in this work on the stepped Co,Os, and Ru (10–16) surface(s). Data in this figure is identical to that in Figs. 3, 4, and 5, but shown aligned together to help guide the eye to similarities and differences. Data are grouped by adsorbate, on each surface. Figure SI3 and SI.4 show this same data, but grouped by site, and by surface/species, respectively. a) For the Co(10–16) surface, b) for the Os(10–16) surface c) for the Ru (10–16) surface.

on each of the surfaces. H_2 and O_2 appear to be the most generally favorable species to find relatively low energy adsorption sites on the terrace under the step edges; this is likely caused by the fact they can adsorb flat (parallel) to the surface at the terrace locations.

Among the species studied on all the surfaces in this work, the species least sensitive to the possible binding site(s) were: H, and CO (Os exception), and OH. Among the species most sensitive to the possible binding site(s) were: C, SO, N, and CH. This might help explain why although Ru is a generally versatile catalyst for many processes, Co and Os are generally less robust and inefficient as general catalysts compared to Ru.

3.5. *Differences across all surfaces: Co* $(10\bar{1}6)$*, Os*$(10\bar{1}6)$*, Ru*$(10\bar{1}6)$

The Co, Os, and Ru $(10\bar{1}6)$ have some marked differences despite the similarities and trends discussed in the preceding sub-section §3.4. The most important difference is that the surfaces as a whole show a disparate range of differences between the min of the B5–B vs B5-A, max of the B5–B vs B5-A, and overall average and standard deviation across all sites. This data can be seen in Tables SI.1, through SI.3 of the Supplementary Information ('rankin-hcp-heliyon-SI.pdf '), but is also summarized as follows: the difference between the min of the B5–B and B5-A goes as -0.23, -0.11, -0.25 and eV for Co, Os, and Ru respectively; the difference between the min of the B5–B and B5-A goes as -0.39, 0.06, -0.06 and eV for Co, Os, and Ru respectively; and the difference between the min of the B5–B and B5-A goes as 0.69, 0.80, 0.67 and eV for Co, Os, and Ru respectively. Therefore, statistically, the Co and Ru favor the B5–B step edge much more strongly than the Os surface, and the average penalty for binding to the sites which are not the lowest energy is much larger on the Os surface. This observation is significantly influenced by the fact that the site 6 on the Os surface behaves much differently for CO* and SO* than the similar site on the Co and Ru surfaces. The final major difference observed between the surfaces studied is that the Os surface behaves qualitatively different than Co and Ru for O_2 adsorptions; specifically, with the lowest energy adsorption site being atop the B5-A step edge atom. For all catalyst surfaces studies in this work, as a general rule, they share nothing in common for the adsorption energetic preferences and trends for the diatomic species other than a small trend for OH.

4. Conclusions

Plane-wave DFT calculations were performed to investigate and determine similarities, tends, and differences in the relative adsorption energies, $\Delta E ads_i$, for the following adsor-bates on the stepped $(10\bar{1}6)$ surface(s) of Co, Os, and Ru. Results indicate that for most of the adsorbates studied, across most of the surfaces, that the B5–B step edge and its local environment provides lower energy adsorption sites. Statistical analysis was performed to categorize various average and standard deviation properties of the adsorbates on each sur-face and site type; there can be large gaps (0.5 eV or more) for the lowest energy sites on each type of step edge (B5–B vs B5-A) however the average is closer to 0.10 eV in preference for all surfaces and adsorbates. Our results show that both of the B5–B and B5-A type step edge site and their local environments are energetically preferred to the nearby terrace site for almost all surfaces and adsorbates; these results are in line with recent literature results for active site determination of nanoparticles of HCP metals used in catalysis. Our use of the surface was found to be a novel tool to characterize the adsorption energies on the two competing step edge types in a fully self-consistent calculation framework. Based on our results, it can be concluded the use of the $(10\bar{1}6)$ surface (or similar related surfaces) should be considered in future studies for adsorption for catalytically relevant adsorbate species on the surface of HCP nanoparticles instead of the legacy technique of creating *ad-hoc* stepped surfaces via manual deletion of atoms from a calculation cell.

Declarations

Author contribution statement

Rees Rankin: Conceived and designed the experiments; Performed the experiments; Analyzed and interpreted the data; Contributed reagents, materials, analysis tools or data; Wrote the paper.

Funding statement

This work was supported by the Department of Chemical Engineering, Villanova University, and the College of Engineering at Villanova University.

Competing interest statement

The authors declare no conflict of interest.

Additional information

Supplementary content related to this article has been published online at https://doi.org/10.1016/j.heliyon.2019.e01924.

Acknowledgements

The authors acknowledge assistance from the Villanova UNIT team for computer support during the execution of this research project. The authors declare/acknowledge there are no conflicts of interest or competing concerns with this research or its publication.

Data availability

The raw data required to reproduce these findings cannot be shared at this time as the data also forms part of an ongoing study. The processed data required to reproduce these findings are available to download as an attachment from rb.rankin@villanova.edu by request.

References

[1] V. Viswanathan, H.A. Hansen, J. Rossmeisl, J.K. NØrskov, Universality in oxygen reduction elec- trocatalysis on metal surfaces, ACS Catal. 2 (8) (2012) 1654–1660.
[2] F. Calle-Vallejo, D. Loffreda, M.T.M. Koper, P. Sautet, Introducing structural sensitivity into ad- sorption–energy scaling relations by means of coordination numbers, Nat. Chem. 7 (2015) 403. https://www.nature.com/articles/nchem.2226#supplementary-information.
[3] F. Calle-Vallejo, J.I. Martínez, J.M. García-Lastra, J. Rossmeisl, M.T.M. Koper, Physical and chemical nature of the scaling relations between adsorption energies of atoms on metal surfaces, Phys. Rev. Lett. 108 (2012) 116103.
[4] A.A. Latimer, A.R. Kulkarni, H. Aljama, J.H. Montoya, J.S. Yoo, C. Tsai, F. Abild-Pedersen, F. Studt, J.K. NØrskov, Understanding trends in C–H bond acti- vation in heterogeneous catalysis, Nat. Mater. 16 (2016) 225. https://www.nature.com/articles/nmat4760#supplementary-information.
[5] J.H. Montoya, C. Tsai, A. Vojvodic, J.K. NØrskov, The challenge of electrochemical Ammonia synthesis: a new perspective on the role of nitrogen scaling relations, ChemSusChem 8 (13) (2015) 2180–2186.
[6] Y. Yan, B.Y. Xia, B. Zhao, X. Wang, A review on noble-metal-free bifunctional heterogeneous catalysts for overall electrochemical water splitting, J. Mater. Chem. 4 (2016) 17587–17603.
[7] G. Xue-Qing, R. R, H. P, CO dissociation and O removal on Co(0001): a density functional theory study, Surf. Sci. 562 (1) (2004) 247–256.
[8] M.A. Petersen, J.-A. van den Berg, I.M. Ciobîcă, P. van Helden, Revisiting CO activation on Co catalysts: impact of step and kink sites from DFT, ACS Catal. 7 (3) (2017) 1984–1992.
[9] J. Liu, D. Hibbitts, E. Iglesia, Dense CO adlayers as enablers of CO hydrogenation turnovers on Ru surfaces, J. Am. Chem. Soc. 139 (34) (2017) 11789–11802.
[10] Y.-H. Zhao, J.-X. Liu, H.-Y. Su, K. Sun, W.-X. Li, A first-principles study of carbon–oxygen bond scission in multiatomic molecules on flat and stepped metal surfaces, ChemCatChem 6 (6) (2014) 1755–1762.
[11] E.T. Nikolaos, Magnus RØnning, B. Øyvind, R. Erling, H. Anders, Deactivation of cobalt based Fischer–Tropsch catalysts: a review, Catal. Today 154 (3) (2010) 162–182.
[12] A.W. Budiman, S.-H. Song, T.-S. Chang, C.-H. Shin, M.-J. Choi, Dry reforming of methane over cobalt catalysts: a literature review of catalyst development, Catal. Surv. Asia 16 (4) (2012) 183–197.
[13] H. Matej, B. Ana, G. Miha, L. Blaž, First-principles mechanistic study of ring hydrogenation and deoxygenation reactions of eugenol over Ru(0001) catalysts, J. Catal. 358 (2018) 8–18.
[14] L. Foppa, C. Copéret, A. Comas-Vives, Increased back-bonding explains step-edge reactivity and particle size effect for CO activation on Ru nanoparticles, J. Am. Chem. Soc. 138 (51) (2016) 16655–16668.
[15] H.-C. Tsai, Y.-C. Hsieh, T.H. Yu, Y.-J. Lee, Y.-H. Wu, B.V. Merinov, P.-W. Wu, S.-Y. Chen, R.R. Adzic, W.A. Goddard, DFT study of oxygen reduction reaction on Os/Pt core–shell catalysts val- idated by electrochemical experiment, ACS Catal. 5 (3) (2015) 1568–1580.
[16] C. Rafael, M.P. Juana, J.R. Diego, Osmium impregnated on magnetite as a heterogeneous cat- alyst for the syn-dihydroxylation of alkenes, Appl. Catal. Gen. 470 (2014) 177–182.
[17] L. Liu, M. Yu, Q. Wang, B. Hou, Y. Liu, Y. Wu, Y. Yang, D. Li, Insight into the structure and morphology of Run clusters on Co(111) and Co(311) surfaces, Catal. Sci. Technol. 8 (2018) 2728–2739.
[18] J.-X. Liu, H.-Y. Su, D.-P. Sun, B.-Y. Zhang, W.-X. Li, Crystallographic dependence of CO activation on cobalt catalysts: HCP versus FCC, J. Am. Chem. Soc. 135 (44) (2013) 16284–16287.
[19] Q. Chen, I.-H. Svenum, Y. Qi, L. Gavrilovic, D. Chen, A. Holmen, E.A. Blekkan, Potassium adsorption behavior on hcp cobalt as model systems for the Fischer–Tropsch synthesis: a density functional theory study, Phys. Chem. Chem. Phys. 19 (19) (2017) 12246–12254.
[20] I.M. Ciobica, R.A. van Santen, Carbon monoxide dissociation on planar and stepped Ru(0001) surfaces, J. Phys. Chem. B 107 (16) (2003) 3808–3812.
[21] Q. Ge, M. Neurock, H.A. Wright, N. Srinivasan, A first principles study of carbon carbon coupling over the 0001 surfaces of Co and Ru, J. Phys. Chem. B 106 (11) (2002) 2826–2829.
[22] S. Shetty, A.P.J. Jansen, R.A. van Santen, Active sites for N2 dissociation on Ruthenium, J. Phys. Chem. C 112 (46) (2008) 17768–17771.
[23] S. Shetty, A.P.J. Jansen, R.A. van Santen, Theoretical investigation of NO dissociation on Ru(1121) surface and nanoparticle, J. Phys. Chem. C 113 (46) (2009) 19749–19752.
[24] Z. Jian-Min, W. Dou-Dou, X. Ke-Wei, Calculation of the surface energy of hcp metals by us- ing the modified embedded atom method, Appl. Surf. Sci. 253 (4) (2006) 2018–2024.
[25] R. Agrawal, P. Phatak, L. Spanu, Effect of phase and size on surface sites in cobalt nanoparticles, Catal. Today 312 (2018) 174–180.
[26] F.R. García-García, A. Guerrero-Ruiz, I. Rodríguez-Ramos, Role of B5-type sites in Ru catalysts used for the NH3 decomposition reaction, Top. Catal. 52 (6) (2009) 758–764.
[27] Z.-P. Liu, P. Hu, General rules for predicting where a catalytic reaction should occur on metal surfaces: a density functional theory study of C H and C O bond breaking/making on flat, stepped, and kinked metal surfaces, J. Am. Chem. Soc. 125 (7) (2003) 1958–1967.
[28] Q. Ge, M. Neurock, Adsorption and activation of CO over flat and stepped Co surfaces: a first principles analysis, J. Phys. Chem. B 110 (31) (2006) 15368–15380.
[29] I. Materials Design, materialsdesign.com. URL materialsdesign.com.
[30] G. Kresse, J. Hafner, Ab initio molecular-dynamics simulation of the liquid-metal-amorphous- semiconductor transition in germanium, Phys. Rev. B 49 (20) (1994) 14251.
[31] G. Kresse, J. Hafner, Ab initio molecular dynamics for open-shell transition metals, Phys. Rev. B 48 (17) (1993) 13115.
[32] G. Kresse, J. Hafner, Ab initio molecular dynamics for liquid metals, Phys. Rev. B 47 (1) (1993) 558.
[33] G. Kresse, J. Furthmüller, Efficient iterative schemes for ab initio total-energy calculations using a plane-wave basis set, Phys. Rev. B 54 (16) (1996) 11169.
[34] G. Kresse, J. Furthmüller, Efficiency of ab-initio total energy calculations for metals and semiconductors using a plane-wave basis set, Comput. Mater. Sci. 6 (1) (1996) 15–50.
[35] B. Hammer, L.B. Hansen, J.K. NØrskov, Improved adsorption energetics within density-functional theory using revised Perdew-Burke-Ernzerhof functionals, Phys. Rev. B 59 (1999) 7413–7421.
[36] M. Methfessel, A.T. Paxton, High-precision sampling for Brillouin-zone integration in metals, Phys. Rev. B 40 (6) (1989) 3616.